

Simple synthetic route for hydroxyapatite colloidal nanoparticles via a Nd:YAG laser ablation in liquid medium

Sung Wook Mhin · Jeong Ho Ryu · Kang Min Kim ·
Gyeong Seon Park · Han Wool Ryu · Kwang Bo Shim ·
Takeshi Sasaki · Naoto Koshizaki

Received: 9 February 2009 / Accepted: 30 March 2009 / Published online: 11 April 2009
© Springer-Verlag 2009

Abstract Pulsed laser ablation (PLA) in liquid medium was successfully employed to synthesize hydroxyapatite (HAp) colloidal nanoparticles. The crystalline phase, particle morphology, size distribution and microstructure of the HAp nanoparticles were investigated in detail. The obtained HAp nanoparticles had spherical shape with sizes ranging from 5 to 20 nm. The laser ablation and the nanoparticle forming process were studied in terms of the explosive ejection mechanism by investigating the change of the surface morphology on target. The stoichiometry and bonding properties were studied by using XPS, FT-IR and Raman spectroscopy. A molar ratio of Ca/P of the prepared HAp nanoparticles was more stoichiometric than the value reported in the case of ablation in vacuum.

PACS 87.85.J- · 81.07.Bc · 79.20.Ds

S.W. Mhin · K.B. Shim
Division of Materials Science and Engineering, Hanyang
University, 17 Haengdang-Dong, Seongdong-Gu, Seoul 133-791,
South Korea

J.H. Ryu (✉) · G.S. Park · H.W. Ryu
Corporate Research Institute, Samsung Electro-Mechanics Co.,
Ltd., 314, Maetan3-Dong, Yeongtong-Gu, Suwon,
Gyeonggi-Do 443-743, South Korea
e-mail: jimihen.ryu@samsung.com
Fax: +82-31-3007900

K.M. Kim
The Institute of Scientific and Industrial Research, Osaka
University, Ibaraki, Osaka 567-0047, Japan

T. Sasaki · N. Koshizaki
High Interface Area Nanostructure Group, Nanotechnology
Research Institute (NRI), National Institute of Advanced
Industrial Science and Technology (AIST), Tsukuba Central 5,
1-1-1 Higashi, Tsukuba, Ibaraki 305-8565, Japan

1 Introduction

Calcium phosphates, notably hydroxyapatite (HAp, $\text{Ca}_{10}(\text{PO}_4)_6(\text{OH})_2$) has attracted a lot of interest due to its similarity with mineral bone. HAp, which is very similar to hard tissue of the human body, shows excellent biocompatibility and bioactivities with respect to human hard tissues. In addition, it has been widely used not only as a biomedical implant material, but also as a drug delivery system and for DNA isolation [1]. Previous studies reported that 20–50 nm HAp nanoparticles play an important role in biomineral formation. It is suggested that the basic inorganic building blocks of tooth and bone may be these nanosized apatite particles [2]. Tens to hundreds of these nanoblocks combine into self-assembled biomaterials with collagen matrix or cells reacted with non-apatitic highly reactive labile ions such as CO_3^{2-} , PO_4^{3-} , HPO_4^{2-} on the cell-material interface, and they show unique physicochemical features such as mechanical strength, insensitivity to growth/dissolution and flexible structure [3–5]. These unique properties depend on the morphology and size of the HAp. For aiming at better and more effective biomedical applications, development of novel synthetic routes for nanosized HAp is very important.

Various approaches have been introduced for the preparation of HAp nanoparticles and their functionalization [6, 7]. Conventionally, solid state reaction, acid-base, precipitation, hydrothermal and sol-gel methods were used for synthesis of HAp powders [8–10]. However, those methods need a long reaction time and several process steps for fabrication. Also, chemical additives in the procedure may be incorporated to HAp particles as impurities, which results in a bad influence on the human body clinically [11, 12]. One novel technique for fabrication of HAp nanoparticles is pulsed laser ablation (PLA) in liquid medium. PLA of solid target in liquid has been a promising technique for producing nanopar-

ticles for analytical and bioanalytical applications as well as rapid synthesis of complex materials because the experimental procedure is simple and above all, a chemical additive is unnecessary [13–15]. However, to date, there have been few reports on the preparation of HAp nanoparticles by laser ablation in liquid medium.

The laser ablation of solids in a liquid medium occurs when a high-power laser beam is focused at the submerged target surface for an appropriate time, and leads to ejection of nanoparticles into the liquid where they are condensed and cooled. Molecular dynamics simulations have proposed two different mechanisms of particle removal during laser ablation [16, 17]. Below a given threshold of laser fluence, there is desorption of small clusters. However, above this threshold of laser fluence, the ejected plume contains a substantial fraction of large molecular clusters due to the thermally induced explosive ejection of the target material.

In this study, we report a novel synthetic approach to produce pure HAp nanoparticles using PLA in liquid medium without any surfactant. The fabricated HAp nanoparticles were characterized in terms of their crystallinity, microstructure and bonding property. Moreover, the laser ablation process was discussed by a thermally induced explosive ejection mechanism.

2 Experimental

The laser ablation process in liquid medium has been well illustrated in the previous literature [13–15]. HAp target (CELLYARD™ pellet, PENTAX) was fixed on the bottom of the glass vessel containing 5 ml high purity distilled water and the target was irradiated by a Nd:YAG pulse laser (repetition rate of 30 Hz, pulse width of 5–7 ns, maximum output of 60 mW) with third harmonic wavelength (355 nm). The laser beam was focused with a single quartz lens of a nominal focal length of 250 mm. The combination of a small input beam size and long focal length lens results in a small focusing angle of $\sim 1^\circ$, which minimizes the possibility of nonlinear absorption in the water above the target [18]. The laser fluence in the range of 10 J/cm^2 was set by fixing the diameter of the laser spot at 1 mm.

The target was rotated during laser ablation to avoid deep ablation traces by continuous irradiation of laser beam. The laser ablation to the HAp target was carried out for 1 hour at room temperature. The morphology of the target before and after laser ablation in de-ionized water was analyzed by a field emission scanning electron microscope (Hitachi S-4800). The prepared colloidal suspension was dropped on a copper mesh coated with amorphous carbon film for observation of microstructure and particle morphology using transmission electron microscopy (JEOL JEM-2010). The size of the nanoparticles was statistically analyzed using

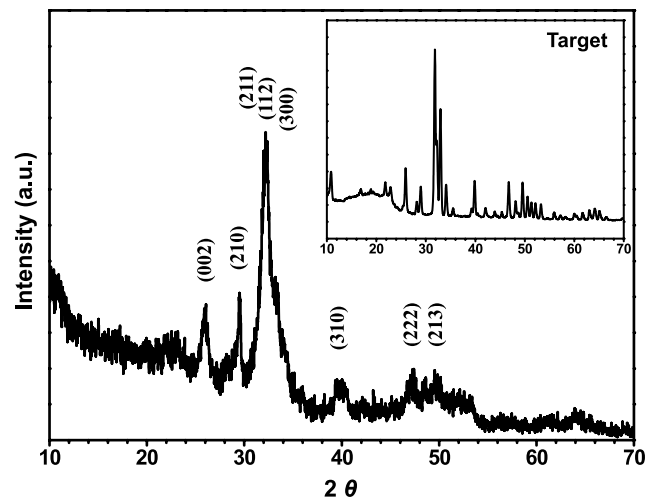


Fig. 1 X-ray diffraction patterns of the HAp nanoparticles collected from the colloidal suspension. The XRD pattern of the target is shown in the *inset*

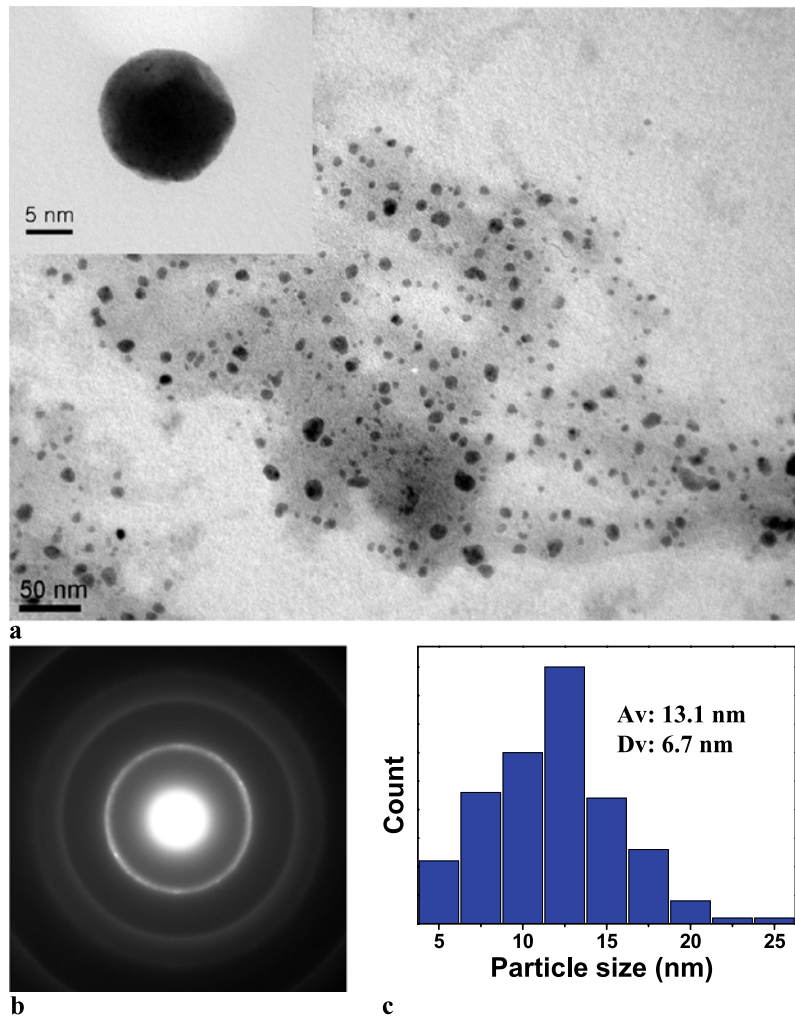
150 nanoparticles in the image of transmission electron microscopy (JEOL JEM-2010). The precipitates of colloidal suspension were prepared for the X-ray diffraction (XRD; Rigaku RAD-C, Cu $K\alpha$ radiation) measurement, X-ray photoelectron spectroscopy (XPS; Perkin-Elmer PHI-5600ci) and Raman spectroscopy (LabRam HR) analysis.

3 Results and discussion

Figure 1 shows XRD pattern of the HAp nanoparticles collected from a colloidal suspension prepared by PLA in de-ionized water. The Bragg reflection peaks of the nanoparticles were indexed well to the hexagonal structured $\text{Ca}_{10}(\text{PO}_4)_6(\text{OH})_2$ in $P6_3m$ space group (JSPDS No. 09-0432). The XRD analysis indicated that the prepared HAp nanoparticles did not contain any discernible crystalline impurity such as β -tricalcium phosphate (β -TCP). The HAp sample had relatively broad XRD peaks compared to the sintered target (inset of Fig. 1), which means the formation of nanoparticles.

The particle morphology, particle size and crystallinity were investigated more closely by TEM as shown in Fig. 2(a). The morphology of the nanoparticles was spherical and uniform with diameters between 5 and 25 nm. Although some particles may look faceted, most of the particles had a sphere-like morphology, which could be clarified by a highly magnified TEM picture as shown in the inset of Fig. 2(a). Selected area electron diffraction (SAED) patterns shown in Fig. 2(b) revealed bright polycrystalline diffraction rings without preferred orientation, and lattice spacings derived from the diffraction rings were in agreement with the hexagonal structured HAp nanoparticles. The particle size distribution shown in Fig. 3(c) was analyzed statistically by

Fig. 2 (a) Typical TEM micrograph of prepared HAp colloidal nanoparticles and (b) corresponding electron diffraction patterns. A highly magnified TEM picture is shown in the inset of Fig. 2(a). (c) Size distribution of the prepared HAp nanoparticles, where A_v and SD represent the average and standard deviation value



random measuring crystal diameters of 150 nanoparticles in sight on the TEM image obtained. During the measurement, no individual particle larger than 30 nm in size was found. The average nanoparticle size was 13.1 nm with a standard deviation of 6.7 nm.

Investigation of the surface morphology of PLA target is the best tool available to identify how particles are formed during laser ablation in liquid medium. The surface morphology change of the HAp target during laser ablation in de-ionized water is shown in Fig. 3. After laser ablation, the surface roughness increased dramatically as seen in Fig. 3(b). When HAp is ablated in vacuum or low pressure gas for film deposition, it was reported that mainly micron size particles were formed. This was explained by propagation of cracks that caused chipping of the micron scale particles [19, 20]. However, in this case, the particles formed in liquid medium by laser ablation are sphere-like uniform nanoparticles with an average diameter of 13.1 nm. The size and shape of the particles indicate that crack propagation theory cannot be applied to the case of PLA in liquid medium. Therefore, we propose an explosive ejection the-

ory, which is one of the standard two models for ablation in the interface between solid and liquid.

According to previous research of laser ablation in the interface between solid and liquid, two primary mechanisms for particle formation by pulsed laser ablation have been identified: thermal vaporization and explosive ejection [21]. In thermal vaporization, laser-induced plasma generated on a target in liquid confines species of atoms, ions and clusters with high energy. In the plasma induced by a laser in liquid medium, the temperature and pressure can climb up instantly to 10^5 K and a few GPa range, respectively [22, 23]. Those species with high energy can react and are quenched, when they contact with molecules of liquid medium, which induces nuclei of oxide or hydroxide via instantaneous hydrothermal oxidation [24]. However, in the case of laser ablation due to thermal vaporization, the surface of the target should be more flat and less rough than in the case of explosive ejection [25, 26]. It seems that this is not the case here. On the other hand, in explosive ejection, the molten droplets from nanometer to micrometer size are ejected directly from the target. The explosive ejection of molten droplet directly

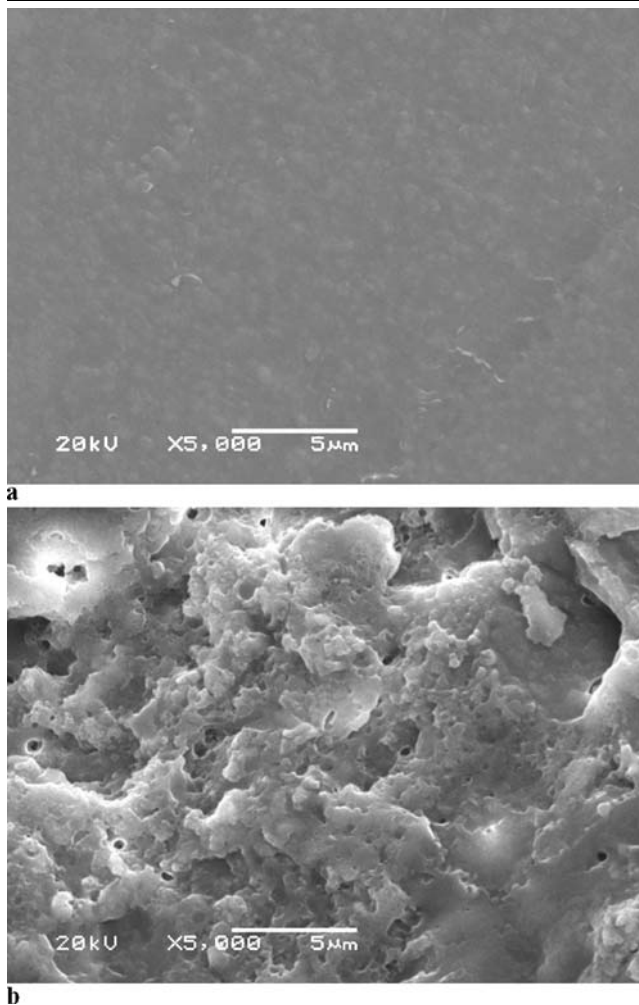


Fig. 3 Typical SEM micrographs of the HAp target (a) before and (b) after laser ablation showing the remarkable change of the surface morphology induced by PLA

from the target is important for nanomaterial synthesis in PLA, because it avoids incongruent vaporization of multi-element targets and the stoichiometry of the target can be preserved in the nanomaterials [22].

In Fig. 3(b), the trace of explosive ejection phenomenon can be observed easily on the HAp target used in PLA. When a target is heated more rapidly than dissipation of heat, the surface of target can pass its boiling point to the metastable superheated region, even in liquid phase. As the temperature reaches the thermodynamic critical temperature, the rate of homogeneous bubble nucleation is increased and the surface of the target transits rapidly from a superheated region to equilibrium liquid droplets [25, 26]. This is called explosive boiling or ejection, which explains the formation of the sphere-like HAp nanoparticles well during laser ablation in de-ionized water.

The surface composition of the HAp nanoparticles collected from the colloidal suspension was analyzed using XPS. A typical survey XPS spectrum from the HAp

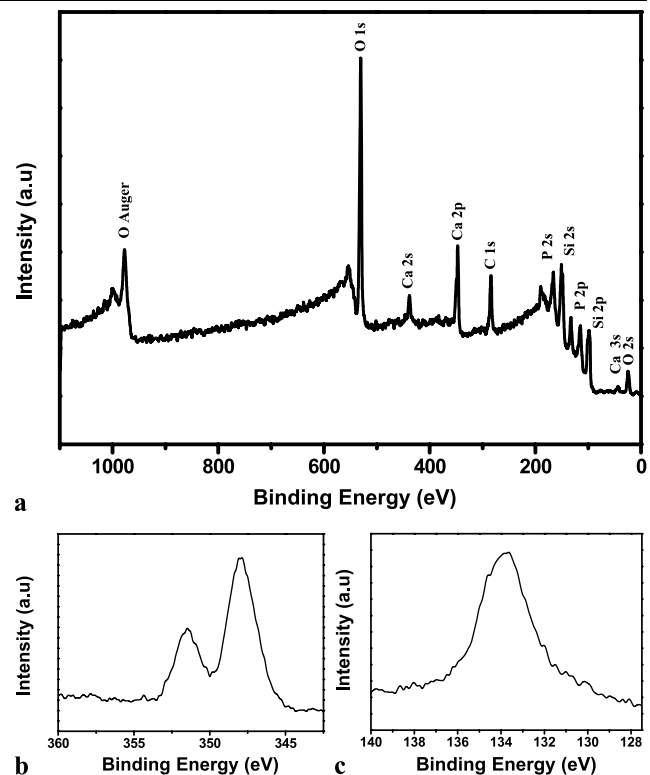


Fig. 4 (a) XPS survey scan spectrum of the HAp nanoparticles and high resolution spectra of (b) Ca (2p) and (c) P (2p) regions

nanoparticles is shown in Fig. 4(a). Besides the expected Ca, P and O peaks, a small C (1s) peak was observed. This carbon is so-called adventitious carbon induced by adsorption of impurity hydrocarbons and is used for binding energy calibration by setting its binding energy to 284.6 eV to correct for sample charging [27]. Other peaks at 99.6 and 150.7 eV are induced by the Si substrate. Figure 4(b, c) show the high resolution XPS spectra of the Ca (2p) and P (2p) regions of the HAp nanoparticles. The binding energy of Ca (2p) was 347.5 and 352.2 eV, and that of P was 133.7 eV. The binding energy values of Ca and P are well in agreement with reported values [28, 29]. A molar ratio of Ca/P calculated from the ratio of the integrated intensity of the Ca to P lines was 2.1, which is approximately 20% higher than the stoichiometric molar ratio of 1.67. A previous study on laser ablation of HAp in vacuum showed the Ca/P molar ratio to rise up to about 3.0 [20]. Hence, it is considered that laser ablation in liquid medium better preserves the chemical composition of the HAp nanoparticles than the laser ablation in vacuum.

Figure 5(a) displays the FT-IR spectrum collected from the HAp nanoparticles prepared by PLA in de-ionized water. The set of absorption bands agrees fairly well with the reported FT-IR data for pure HAp [30, 31]. A set of characteristic bands representing apatitic PO_4^{3-} groups is observed at $1090, 1050 \text{ cm}^{-1}$ (ν_3 triply degenerated asymmetric stretch-

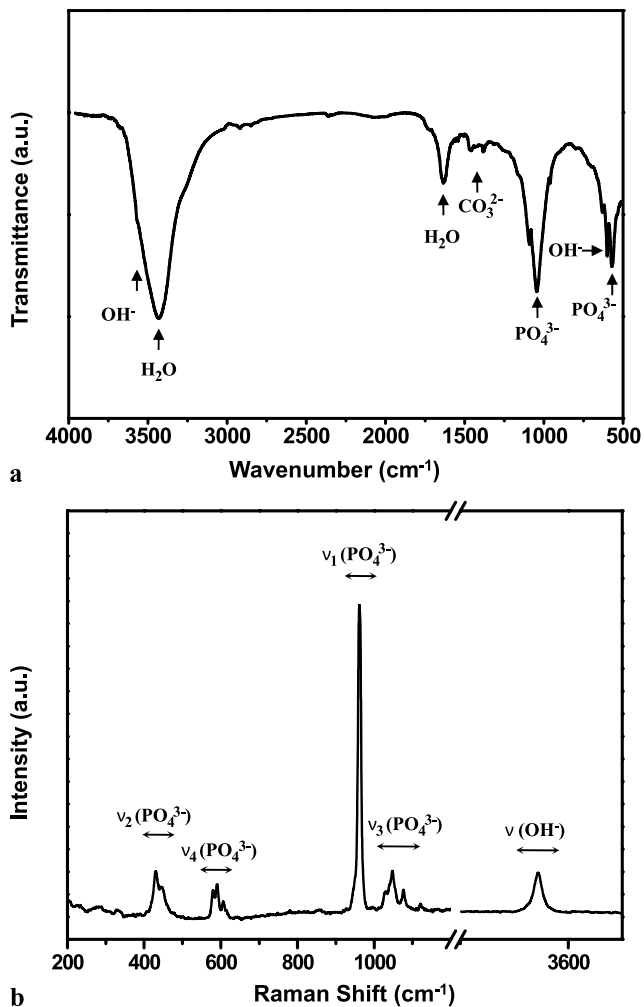


Fig. 5 (a) FT-IR and (b) Raman scattering spectrum of the HAP nanoparticles prepared by PLA in de-ionized water

ing mode of the P–O bond) and 960 cm^{-1} (ν_1 symmetric stretching mode of the P–O bond). Additional absorption bands representing a ν_4 triply degenerated bending mode of the O–P–O bond at 570 cm^{-1} are also observed in the low wavenumber region. The broad band at $3300\text{--}3600\text{ cm}^{-1}$ corresponds to adsorbed water and stretching vibration (ν_s) of the lattice structural hydroxyl anions. The weak peak at 610 and 1640 cm^{-1} is assigned to the librational mode (ν_L) and bending mode (ν_2) of the lattice OH^- ions. In particular, the peaks observed at 1490 and 1430 cm^{-1} are attributed to carbonate (CO_3^{2-}) traces partially occupying OH^- positions.

Figure 5(b) shows the Raman scattering spectrum of the prepared HAP nanoparticles. The band positions are in good agreement with published data on bulk HAP powder [32, 33]. The spectrum represents a very intense characteristic peak at 960 cm^{-1} owing to the symmetric stretching mode $\nu_1(\text{PO}_4^{3-})$. Apart from this ν_1 mode, the other stretching modes of the PO_4^{3-} groups are also observed, namely,

ν_2 at 440 cm^{-1} , ν_4 at 590 cm^{-1} , and ν_3 at the 1050 cm^{-1} region. The broad band at 3570 cm^{-1} corresponds to the stretching vibration of the hydroxyl groups.

4 Conclusion

Hydroxyapatite (HAp, $\text{Ca}_{10}(\text{PO}_4)_6(\text{OH})_2$) colloidal nanoparticles were successfully synthesized via a simple synthetic route using a Nd:YAG pulsed laser ablation (PLA) in de-ionized water without any surfactant. The obtained HAP nanoparticles were phase pure and highly crystalline with uniform spherical shape. The average particle size was 13.1 nm with a standard deviation of 6.7 nm . The explosive ejection mechanism could explain the formation process of crystalline HAP nanoparticles well, by which the molten droplets are ejected directly from the target during laser ablation. The surface composition (Ca/P ratio) of the HAP nanoparticle prepared by PLA in liquid was relatively more stoichiometric than the composition reported for HAP prepared in vacuum. These results confirm that the PLA in liquid medium can be a synthetic route for biomedical materials.

References

1. A.A. Chaudhry, S. Haque, S. Kellici, P. Boldrin, I. Rehman, F.A. Khalid, J.A. Darr, *Chem. Commun.* 2286 (2006)
2. R.K. Tang, L.J. Wang, C.A. Orme, T. Bonstein, P.J. Bush, G.H. Nancollas, *Angew. Chem. Int. Ed.* **43**, 2697 (2004)
3. A.P. Alivisatos, *Science* **289**, 736 (2000)
4. A. Boskey, *Osteoporos. Int.* **14**, 16 (2003)
5. J.D. Pateris, B. Wopenka, J.J. Freeman, K. Rogers, E. Valsami-Jones, J.A.M. van der Houwen, M.J. Silva, *Biomaterials* **25**, 229 (2004)
6. D. Walsh, J.L. Kingston, R. Heywood, S.J. Mann, *J. Cryst. Growth* **133**, 1 (1993)
7. M. Gonzalez-Mcguire, J.-Y. Chane-Ching, E. Vignaud, A. Lebugle, S.J. Mann, *J. Mater. Chem.* **14**, 2277 (2004)
8. H.-M. Kim, Y. Kim, S.-J. Park, C. Rey, H. Lee, M.J. Glimcher, J.S. Ko, *Biomaterials* **21**, 1129 (2000)
9. S. Bose, S.K. Saha, *Chem. Mater.* **15**, 4464 (2003)
10. N. Yamasaki, T. Kai, M. Nishioka, K. Yanagisawa, K. Ioku, *J. Mater. Sci.* **9**, 1150 (1990)
11. J.R. Wright, *Physiol. Rev.* **77**, 931 (1997)
12. M. Griese, *Eur. Respir. J.* **13**, 1445 (1999)
13. A. Henglein, *J. Phys. Chem.* **97**, 5457 (1993)
14. C.H. Liang, Y. Shimizu, M. Masuda, T. Sasaki, N. Koshizaki, *Chem. Mater.* **16**, 963 (2004)
15. G.S. Park, K.M. Kim, S.W. Mhin, J.W. Eun, K.B. Shim, J.H. Ryu, N. Koshizaki, *Electrochem. Solid-State Lett.* **11**, J23 (2008)
16. M.S.F. Lima, F.P. Ladário, R. Riva, *Appl. Surf. Sci.* **252**, 4420 (2006)
17. J.H. Ryu, G.S. Park, K.M. Kim, C.S. Lim, J.-W. Yoon, K.B. Shim, *Appl. Phys. A* **88**, 731 (2007)
18. A. Vogel, J. Noack, K. Nahen, D. Theisen, S. Busch, U. Parltitz, D.X. Hammer, G.D. Noojin, B.A. Rockwell, R. Birngruber, *Appl. Phys. B* **68**, 271 (1999)

19. P. Baeri, L. Torrisi, N. Marino, G. Foti, *Appl. Surf. Sci.* **54**, 210 (1992)
20. V.N. Bagratashvili, E.N. Antonov, E.N. Sobol, V.K. Popov, S.M. Howdle, *Appl. Phys. Lett.* **66**, 2451 (1995)
21. W.T. Nichols, T. Sasaki, N. Koshizaki, *J. Appl. Phys.* **100**, 114911 (2006)
22. A. Miotello, R. Kelly, *Appl. Phys. Lett.* **67**, 3535 (1995)
23. L. Berthe, R. Fabbro, P. Peyre, E. Bartnicki, *J. Appl. Phys.* **85**, 7552 (1999)
24. L. Berthe, R. Fabbro, P. Peyre, L. Tollier, E. Bartnicki, *J. Appl. Phys.* **82**, 2826 (1997)
25. L.V. Zhigilei, P.B.S. Kodali, B.J. Garrison, *J. Phys. Chem. B* **102**, 2845 (1998)
26. A.A. Oraevsky, S.L. Jacques, *J. Appl. Phys.* **78**, 1281 (1995)
27. P. Swift, *Surf. Interface Anal.* **4**, 47 (1981)
28. H.B. Lu, C.T. Campbell, D.J. Graham, B.D. Ratner, *Anal. Chem.* **72**, 2886 (2000)
29. S.C. Lee, H.W. Choi, H.J. Lee, K.J. Kim, J.H. Chang, S.Y. Kim, J. Choi, K.-S. Oh, Y.-K. Jeong, *J. Mater. Chem.* **17**, 174 (2007)
30. S. Koutsopoulos, *J. Biomed. Mater. Res.* **62**, 600 (2002)
31. B.O. Fowler, *Inorg. Chem.* **13**, 194 (1974)
32. G.R. Sauer, W.B. Zunic, J.R. Durig, R.E. Wuthier, *Calcif. Tissue Int.* **54**, 414 (1994)
33. H. Tsuda, J. Arends, *J. Dent. Res.* **72**, 1609 (1993)